shown in Fig. 1 caused extensive damage to Greeley, Colorado, 1/2 hour earlier; surface observations of baseball-sized hail were reported by mobile observers with the Prototype Regional Observing and Forecasting Systems of the National Oceanic and Atmospheric Administration (NOAA). Observers were located at the points marked A and B in Fig. 1. Regions of larger positive Z_{DR} surrounding the hail cell are locations where rain fell.

On the evening of 8 June 1983, a severe storm developed near Wiggins, Colorado. Low-elevation PPI scans of Z_H and Z_{DR} are shown in Fig. 2, a and b, respectively. Locations of three hail cells based on the Z_{DR} hail signal are contoured in Fig. 2. Note the clear delineation of hailshafts from rain regions. A range height indicator (RHI) scan at an azimuth of 76° through the same storm at a slightly later time is shown in Fig. 3. The center of the hailshaft occurs approximately at 80-km range, where $Z_H > 55$ dBZ and $Z_{DR} \cong 0$ dB. Regions of rainfall surround the hailshaft and are characterized by $Z_{DR} \gtrsim 0.5$ dB. Note also the discrimination between ice and water phase with height observed with the Z_{DR} signal, a characteristic signature (*23*).

The Z_{DR} radar technique is likely to become an important procedure for the detection of hail in severe storms and in hail suppression research. Although further work is required to demonstrate the utility of this technique in an operational environment, a preliminary assessment based upon the results of Project MAYPOLE and other experiments strongly supports use of the Z_{DR} technique for this purpose (*22, 24*).

V. N. BRINGI
Department of Electrical Engineering, Colorado State University, Fort Collins 80523

THOMAS A. SELIGA
KULTEGIN AYDIN
Atmospheric Sciences Program and Department of Electrical Engineering, Ohio State University, Columbus 43210

References and Notes

1. B. Cook, *Mon. Weather Rev.* **86**, 435 (1958); R. H. Douglas and W. Hitschfeld, Science Report MW-27 (Stormy Weather Group, McGill University, Montreal, 1958); R. J. Donaldson, Jr., A. C. Chmela, C. R. Shackford, in *Physics of Precipitation* (American Geophysical Union, Washington, D.C., 1959), pp. 354–369; R. J. Donaldson, Jr., *J. Meteorol.* **18**, 292 (1961).
2. P. J. Petrocchi, Science Report AFGL-TR-82-0277 (Air Force Geophysics Laboratory, Hanscom Air Force Base, Mass., 1982).
3. R. J. Donaldson, Jr., and D. W. Burgess, in *Proceedings of the NEXRAD Doppler Radar Symposium/Workshop*, P. S. Ray and K. Colbert, Eds. [University of Oklahoma (Norman)–NOAA, Washington, D.C., 1982], pp. 102–123.
4. D. Atlas and F. H. Ludlam, *Q. J. R. Meteorol. Soc.* **87**, 523 (1961).
5. G. K. Sulakvelidze, N. Sh. Bibilashvili, V. F. Lapcheva, *Formation of Precipitation and Modification of Hail Processes* (Israel Program for Scientific Translation, Jerusalem, 1965); G. K. Sulakvelidze, B. I. Kiziriya, V. V. Tsykunov, in *Weather and Climate Modification*, W. N. Hess, Ed. (Wiley, New York, 1974), pp. 410–431; I. I. Burtsev, *Modification of Hail Processes* (Gidrometeoizdat, Leningrad, 1973).
6. D. Atlas, *Adv. Geophys.* **10**, 317 (1964).
7. P. J. Eccles and D. Atlas, *J. Appl. Meteorol.* **12**, 847 (1973).
8. R. E. Rinehart and J. D. Tuttle, *ibid.* **21**, 1865 (1982).
9. G. C. McCormick and A. Hendry, *Radio Sci.* **10**, 421 (1975).
10. B. L. Barge, Science Report MW-71 (Stormy Weather Group, McGill University, Montreal, 1972); G. C. McCormick, L. E. Allan, A. Hendry, *J. Appl. Meteorol.* **18**, 77 (1979); A. Hendry and Y. M. M. Antar, *Radio Sci.* **19**, 115 (1984).
11. R. G. Humphries, thesis, McGill University (1974); Science Report MW-82 (Stormy Weather Group, McGill University, Montreal, 1974); J. I. Metcalf, *Radio Sci.* **16**, 1373 (1981); T. A. Seliga, K. Aydin, V. N. Bringi, *ibid.* **19**, 81 (1984).
12. T. A. Seliga and V. N. Bringi, *J. Appl. Meteorol.* **15**, 69 (1976).
13. R. G. Knollenberg, *ibid.* **9**, 86 (1970).
14. V. N. Bringi, T. A. Seliga, W. A. Cooper, *Radio Sci.* **19**, 157 (1984); W. A. Cooper, V. N. Bringi, V. Chandrasekhar, T. A. Seliga, in Preprints, 21st Conference on Radar Meteorology, Edmonton, Alberta (American Meteorological Society, Boston, 1983), pp. 488–493.
15. G. C. McCormick, A. Hendry, B. L. Barge *Nature (London)* **238**, 214 (1972); K. V. Beard and A. R. Jameson, *J. Atmos. Sci.* **40**, 448 (1983).
16. A. Hendry, G. C. McCormick, B. L. Barge, *J. Appl. Meteorol.* **15**, 635 (1976).
17. H. R. Pruppacher and K. V. Beard, *Q. J. R. Meteorol. Soc.* **96**, 247 (1970); H. R. Pruppacher and R. L. Pitter, *J. Atmos. Sci.* **28**, 86 (1971).
18. A. Hendry and Y. M. M. Antar, *Radio Sci.* **19**, 115 (1984).
19. S. Richardson, B. Barge, R. Humphries, in Preprints, 21st Conference on Radar Meteorology, Edmonton, Alberta (American Meteorological Society, Boston, 1983), pp. 421–424.
20. V. N. Bringi, T. A. Seliga, S. M. Cherry, *IEEE Trans. Geosci. Remote Sensing* **21**, 215 (1983).
21. V. N. Bringi and T. A. Seliga, *Ann. Telecommun.* **32**, 392 (1977); T. A. Seliga and V. N. Bringi, *Radio Sci.* **13**, 271 (1978); K. Aydin and A. Hizal, Union Radio Scientifique Internationale (URSI) National Radio Science Meeting Abstracts, Seattle, Wash., June 1979.
22. T. A. Seliga, K. Aydin, C. P. Cato, V. N. Bringi, in *Cloud Dynamics*, E. M. Agee and T. Asai, Eds. (Reidel, Dordrecht, 1982), pp. 285–300; K. Aydin, T. A. Seliga, V. N. Bringi, *Radio Sci.* **19**, 58 (1984).
23. M. P. M. Hall, S. M. Cherry, J. W. F. Goddard, G. R. Kennedy, *Nature (London)* **285**, 195 (1980).
24. V. N. Bringi, V. Chandrasekhar, T. A. Seliga, P. L. Smith, R. Hari, in Preprints, 21st Conference on Radar Meteorology, Edmonton, Alberta (American Meteorological Society, Boston, 1983), pp. 494–499; M. J. Leitao and P. A. Watson, *Radio Sci.* **19**, 209 (1984).
25. This work was supported by the Atmospheric Research Section, National Science Foundation, under grants ATM-8003376 and ATM-8117045, and by the Army Research Office through the University Corporation for Atmospheric Research subcontracts NCAR S3024 and NCAR S3025. We are grateful to R. E. Carbone, P. H. Herzegh, and other staff members of the Field Observing Facility (NCAR), for their assistance in the conduct of this research during Project MAYPOLE. Cooperation of the mobile observers with NOAA's Prototype Regional Observing and Forecasting Systems group in verifying the hail observations on 4 June 1983 is gratefully acknowledged. Software support for radar data analysis was provided by C. Mohr and L. J. Miller of the Convective Storms Division, NCAR. NCAR is sponsored by the National Science Foundation.

23 February 1984; accepted 10 April 1984

Large Yearly Production of Phytoplankton in the Western Bering Strait

Abstract. *Production in the western Bering Strait is estimated at 324 grams of carbon per square meter per year over 2.12×10^4 square kilometers. An ice-reduced growing season makes this large amount of primary production unexpected, but it is consistent with the area's large upper trophic level stocks. The productivity is fueled by a cross-shelf flow of nutrient-rich water from the Bering Sea continental slope. This phytoplankton production system from June through September is analogous to a laboratory continuous culture.*

Mesoscale spatial patterns in marine productivity usually reflect underlying physical processes that determine phytoplankton growth conditions. In low latitudes, surface divergence is necessary to bring nutrient-containing water into euphotic depths. In high-latitude cold surface waters, nutrients increase during winter when mixed layer light conditions are poor and are seasonally incorporated into plant organic material only under suitable upper water column light and mixing conditions (*1*). Despite these limitations, intense summer productivity in the western Bering Strait creates a large amount of phytoplankton each year.

The eastern Bering Sea is unusual among continental shelves because of its large area and a cross-shelf advection into the Arctic Ocean through the Bering Strait (Fig. 1). Current measurements suggest average flow through the Bering Strait is approximately 0.8 sverdrups (*2*). This flow is seasonal, being greater in summer because of the higher frequency of flow reversals in winter. The water passing through the strait has three major components (*3*). In the west, the flow is dominated by cold, high salinity water from the Gulf of Anadyr. This flow appears to be a continuation of the shelf break current that turns north near Cape Navarin (Fig. 1). In the east, warmer coastal water dominated by Yukon River discharge flows out of Norton Sound. South of Saint Lawrence Island, the third water mass (modified shelf water) is formed. The Bering shelf–Anadyr water in the west and the Alaskan coastal–Yukon River water in the east maintain their identity during transit through the strait.

An important characteristic of the Bering shelf–Anadyr water is its high nutrient content. Chemical data over the last 15 years (*4–9*) all indicate that this western flow is associated with much greater nitrate concentrations than the Alaskan coastal water (Fig. 2). The Bering shelf–Anadyr flow, therefore, continuously supplies nutrients to the shallow Bering Strait. This mechanism of nutrient supply is distinct from that of local upwelling since in the western Bering Strait plume there is a geographic separation of approximately 500 km between the water's source and its biological utilization. In addition, this flow appears to be more consistent in time and space than coastal upwelling (*10*). The nutrient-laden western Bering Strait flow is also associated with a large standing crop of phytoplankton (Fig. 2).

Yearly phytoplankton growth in the western strait however, is limited by the length of time during which suitable water column light conditions prevail. These conditions depend not only on daily light (solid line in Fig. 3) but also on the depth of the surface mixed layer (*11*). In nutrient-replete surface waters, ratios of the mixed layer depth to the critical depth of less than ~0.3 can support several grams of carbon production per square meter per day with daily light levels comparable to Bering Strait summer values (*12*). In the uniformly shallow (~40 to 50 m) Bering Strait area such optimum growth conditions potentially exist from March to September (broken line in Fig. 3). However, ice typically does not leave the strait until June (*13*), which restricts the period conducive to rapid water column phytoplankton growth to June through September.

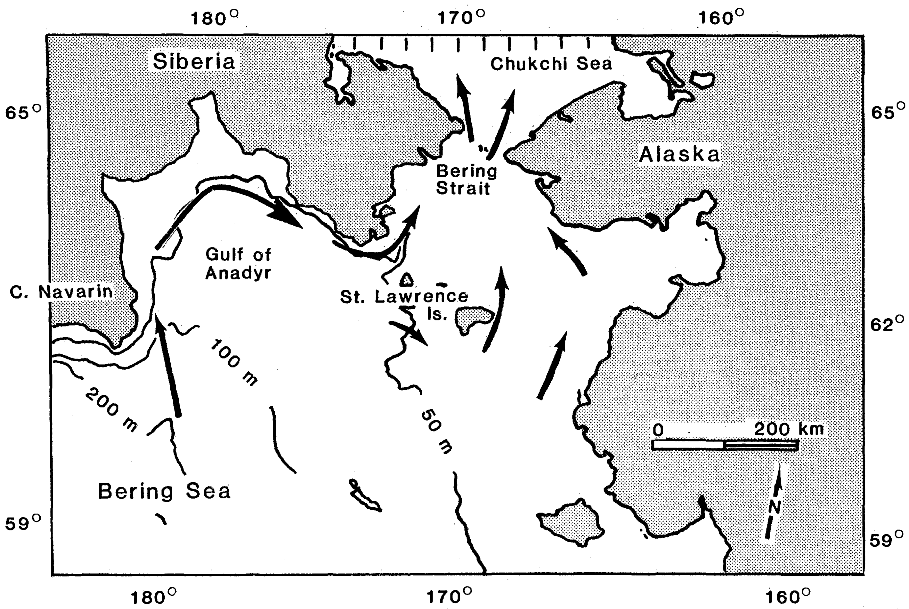

Fig. 1. Map of northern Bering and southern Chukchi Sea regions showing bathymetry and net water movement (*2*). Arrows indicate direction of current.

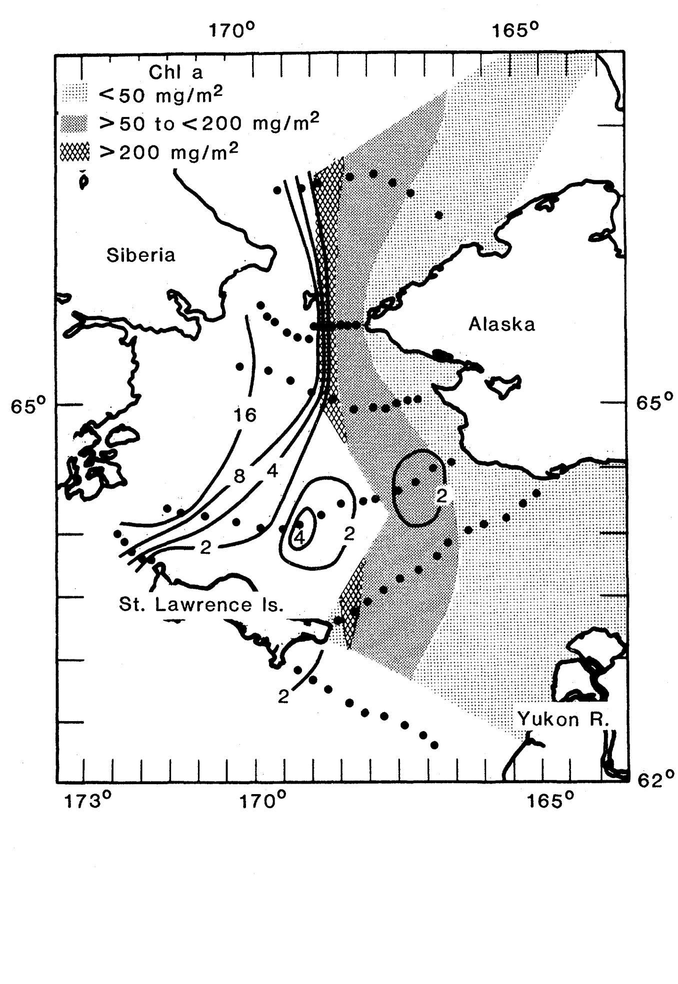

Fig. 2. Composite areal distribution of water column nitrate and chlorophyll a (Chl a) during the summer. Average water column nitrate concentrations (milligram-atoms per cubic meter) are indicated by labeled isopleths. Solid dots indicate nitrate sampling points (*4*). Total water column chlorophyll a content (milligrams per square meter) is indicated by cross-hatched areas (*9*). Sampling points for chlorophyll a (not shown) covered both Norton and Kotzebue sounds. No chlorophyll a data were taken west of 168°W longitude.

In a laboratory continuous culture of algae, favorable growth conditions are maintained by the continuous addition of nutrients and removal of cell yield. We propose that the flow of nutrient-rich Bering shelf–Anadyr water through the western Bering Strait functions much like this model during the summer months (*14*). We use nitrate utilization to follow phytoplankton activity in the western strait as the nitrate from the Bering shelf–Anadyr flow is in some part consumed during its northward movement. This approach is consistent with both the flow regime and nitrate distribution in the area. A simple mass balance relation can then be applied to the production system

$$\rho NO_3^- = \Delta NO_3^- \frac{\text{Flow}}{\text{Area}} \qquad (1)$$

Where ρNO_3^- is the areal nitrate utilization rate (in milligram-atoms per square meter per day), and ΔNO_3^- is the decrease in average water column nitrate concentration through the western Bering Strait [~6 mg-atom m^{-3} (*15*)]. The average summer transport rate in the strait is ~1.3 Sv (*3*), and we estimated the Bering shelf–Anadyr flow, which is about 60 percent of strait transport, with the rest consisting of Alaskan coastal and modified shelf water that was not considered in the calculation. The area, the typical extent of Bering shelf–Anadyr water in the strait, was determined from available oceanographic data (2.12×10^4 km^2).

The resulting nitrate utilization rate for the western Bering Strait is 17.6 mg-atom/m^2 per day. This value approaches rates measured during optimum bloom conditions on the southeastern Bering shelf (*12*). Recent measurements (*9*) indicated nitrate uptake increased from less than 1 mg-atom/m^2per day in Alaskan coastal water to over 5 mg-atom/m^2 per day at the edge of the western plume. Previous measurements in the western flow recorded nitrate uptake rates of more than 20 mg-atom/m^2 per day (*6*).

Carbon production, however, depends on total nitrogen (nitrate plus ammonium) uptake. Measurements of the ratio of new to total nitrogen uptake (the *f* factor) varied from 0.35 at the edge of the plume (*9*) to 0.80 in the middle of the plume (*6*). An average *f* factor of 0.55 was used to estimate the equivalent carbon productivity from the calculated nitrate utilization rate. The resulting estimate for carbon of 2.7 g/m^2 per day is within the range of carbon productivity values measured in this water mass (*16*). Since mixed layer light conditions can support this level of production from June to September, the yearly carbon production in the western flow is approximately 324 g/m^2. This figure does not include fall or epontic algal production. A substantial sedimentary efflux of regenerated nutrients may also occur. While production in the western strait has an unusually low dependence on regenerated nitrogen, it may be important for phytoplankton growth downstream from the strait.

A comparison among several shelf areas indicates that yearly production varies a great deal (Table 1). The large yearly production estimated for the western Bering Strait is unusual considering its Arctic location. Shelves exhibiting large production are areas where physical oceanographic processes keep the euphotic zone supplied with nutrients. This point is illustrated by computing the nutrient supply rate (NSR) for each area

$$\text{NSR} = \frac{\rho\text{NO}_3^- - \text{winter NO}_3^- \text{ store}}{\text{growing season} \times (\text{NO}_3^-)_{\text{bottom water}}} \quad (2)$$

where ρNO_3^- is the yearly amount of nitrate utilization (in milligram-atoms per square meter), and the winter store of nitrate is the amount present in the upper water at the end of winter. The difference must be supplied during the growing season. This supply is normalized to the length of the growing season (days) and the nitrate concentration of the source water (in milligram-atoms per cubic meter), to yield a supply rate (in meters per day). On this basis, it is clear that the physics controlling nutrient supply also control production (Table 1).

In shallow areas of temperate shelves, pelagic zooplankton grazing is often a minor sink for primary production (*17*). The large standing stock of benthic organisms in the Bering Strait (*18*) suggests that much of the "cell yield" of the western Bering Strait system reaches the bottom in this area as well. In addition, the northward flow may deposit some of the organic matter synthesized in the strait in the Chukchi Sea. This deposition is compatible with the elevated organic carbon content found in southern Chukchi Sea sediments (*19*).

Table 1. Comparisons among several shelf production regimes.

Shelf	Yearly production of carbon (g/m^2)	*f* factor*	Growing† season (days)	Nutrient supply rate (m/day)	Benthic flux of carbon (g/m^2)
Georges Bank	375 (*24*)	0.45	240	0.90	200 (*25*)
New York Bight	250 (*25*)	0.42	240	0.45	115 (*25*)
Western Bering Strait	324	0.55	120	0.67	290‡
Southeast Bering Strait	170 (*12*)	0.40	160	0.17	150 (*17*)
(middle shelf), Peru	1000 (*26*)	0.50	365	1.24	200 to 500 (*26*)

*From either the reference indicated or carbon production relation in (*20*). †The length of time a stable, ice-free water column exists. ‡Estimated.

The rapid sedimentation of organic material also influences the biogeochemistry of nutritive elements. There is a relation between the trophodynamic concept of new production and surface ocean carbon loss from the ocean surface (*20*). The western Bering Strait exhibited a marked depression in surface CO_2 partial pressures during summer (*8*), as did the southeast Bering shelf during very productive periods (*21*). The biophysical characteristics of the area, therefore, suggest that it is presently a sink for atmospheric carbon, a role suggested for shelf-slope areas in general (*22*).

Marine production systems are geographically heterogeneous in their ability to remove a large proportion of carbon and nitrogen from active nutrient pools. The western Bering Strait production regime is a good example of a present-day biogeochemical reaction center. It is an area of high primary production, a large amount of nitrate uptake, and a shallow water column. The possible significance of such areas in global elemental cycles raises questions regarding the effects of perturbations. These perturbations range from short time scale anthropogenic influences to longer scale and perhaps more dramatic impacts brought about by eustatic changes in sea level. For example, although several oceanic factors can influence atmospheric CO_2 concentrations, productivity in cold oceans is probably an important determinant (*23*). Modeling of the CO_2 system must reconcile the loss of productive high-latitude shelf areas with the hypothesized increase in marine productivity during glacial periods.

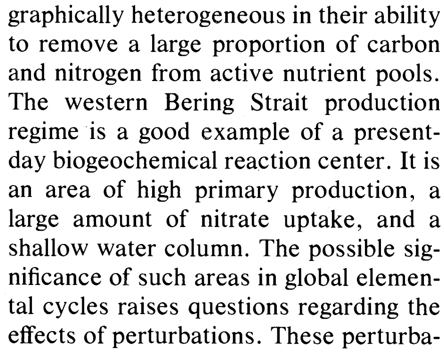

Fig. 3. Seasonal changes in photosynthetically active radiation and the ratio of the mixed layer depth to the critical depth (MLD:CD) in the Bering Strait. Shaded areas indicate ice-covered period.

R. N. SAMBROTTO
J. J. GOERING
C. P. MCROY
Institute of Marine Science, University of Alaska, Fairbanks 99701

References and Notes

1. J. H. Ryther, in *The Sea*. M. N. Hill, Ed. (Interscience, New York, 1963), vol. 2, pp. 347–380.
2. L. K. Coachman and K. Aagaard, in *The Eastern Bering Sea Shelf: Oceanography and Resources*, D. W. Hood and J. A. Calder, Eds. (Univ. of Washington Press, Seattle, 1981), pp. 95–110.
3. L. K. Coachman, K. Aagaard, R. B. Tripp, *Bering Strait: The Regional Physical Oceanography* (Univ. of Washington Press, Seattle, 1975).
4. D. M. Husby and G. L. Hufford, *U.S. Coast Guard Oceanogr. Rep. CG 373–42* (1969).
5. P. J. Kinney, D. C. Burrell, M. E. Arhelger, T. C. Loder, D. W. Hood, *Inst. Mar. Sci. Univ. Alaska Rep. R-70-23* (1970).
6. C. P. McRoy, J. J. Goering, W. E. Shiels, in *Biological Oceanography of the Northern North Pacific Ocean*. A. Y. Takenouti, Ed. (Idemitsu Shoten, Tokyo, 1972), pp. 125–138.
7. K. O. Coyle, "The oceanographic results of the cooperative Soviet-American cruise to the Chukchi and East Siberian seas aboard the Soviet whale-hunting ship *Razvachchii*" (Institute of Marine Science, University of Alaska, Fairbanks, 1981).
8. I. Koiko, K. Furuya, H. Otobe, T. Nakai, T. Memoto, A. Hattori, *Deep Sea Res.* **29**, 149 (1982).
9. C. P. McRoy, "Cruise report, R/V *Alpha Helix* 049, 15–26 August 1983" (Institute of Marine Science, University of Alaska, Fairbanks, 1983).
10. On the basis of measured current speeds in Anadyr Strait (*2*) and an original depth of 150 to 200 m for Bering shelf–Anadyr water, this water rises approximately 8 m/day during its transit to Bering Strait. This is in the range of vigorous upwelling rates.
11. H. U. Sverdrup, *J. Cons. Cons. Int. Explor. Mer* **18**, 287 (1953).
12. R. N. Sambrotto, H. J. Niebauer, J. J. Goering, R. L. Iverson, *Cont. Shelf Res.*, in press.
13. H. J. Niebauer, *J. Geophys. Res.* **85** (C12), 7507 (1980).
14. The analogy serves as a conceptual model only. Natural systems differ significantly from controlled laboratory situations [H. W. Jannasch, *Limnol. Oceanog.* **19** (No. 4), 716 (1974)]. How-

ever, continuous culture models have been applied outside the laboratory [A. F. Gaudy and E. T. Gaudy, *Annu. Rev. Microbiol.* **20**, 319 (1966)].
15. The nitrate concentrations were followed along isohalines from Anadyr Strait to the most northerly section sampled in (*4*), and the average change taken as ΔNO_3^-.
16. A carbon productivity of 2.05 g/m^2 per day was recorded recently at the plume edge (9), and 4.1 g/m^2 per day was measured in the plume center (*6*).
17. M. J. Dagg *et al.*, *Deep-Sea Res.* 29 (1A), 45 (1982).
18. S. Stoker, in *The Eastern Bering Sea Shelf: Oceanography and Resources*. D. W. Hood and J. A. Calder, Eds. (Univ. of Washington Press, Seattle, 1981), pp. 1069–1090.
19. J. J. Walsh, *Prog. Oceanogr.* **12**, 1 (1983).
20. R. W. Eppley and B. J. Peterson, *Nature (London)* **282**, 677 (1979).
21. D. W. Hood, in *The Eastern Bering Sea Shelf: Oceanography and Resources*, D. W. Hood and J. A. Calder, Eds. (Univ. of Washington Press, Seattle, 1981), pp. 347–358.
22. J. J. Walsh, G. T. Rowe, R. L. Iverson, C. P. McRoy, *Nature (London)* **291**, 196 (1981).
23. J. L. Sarmiento and J. R. Toggweiler, *ibid.* **308**, 621 (1984).
24. E. B. Cohen, M. D. Grosslein, M. P. Sissenwine, F. Steimle, W. R. Wright, *Can. Spec. Publ. Fish. Aquat. Sci.* **59**, 95 (1982).
25. M. J. Dagg and J. T. Turner, *Can. J. Fish. Aquat. Sci.* **39**, 979 (1982).
26. J. J. Walsh, *Nature (London)* **290**, 300 (1981).
27. We thank L. Coachman and two anonymous reviewers for helpful comments. Supported by NSF grants DPP-8300916 and DPP-7623340. Contribution 552, Institute of Marine Science, University of Alaska, Fairbanks.

2 April 1984; accepted 16 May 1984

Side-Scan Sonar Assessment of Gray Whale Feeding in the Bering Sea

Abstract. *Side-scan sonar was used to map and measure feeding pits of the California gray whale over 22,000 square kilometers of the northeastern Bering Sea floor. The distribution of pits, feeding whales, ampeliscid amphipods (whale prey), and a fine-sand substrate bearing the amphipods were all closely correlated. The central Chirikov Basin and nearshore areas of Saint Lawrence Island supply at least 6.5 percent of the total gray whale food resource in summer. While feeding, the whales resuspend at least 1.2 × 10^8 cubic meters of sediment annually; this significantly affects the geology and biology of the region.*

The migratory habits of California gray whales (*Eschrichtius robustus*) allow them to be accurately censused (*1*), and their benthic mode of feeding leaves a measurable record of the amount of prey consumed. These factors provide an opportunity to quantify the feeding ecology of gray whales. Primarily coastal-dwelling, the whales calve and breed in lagoons in Baja California in winter and migrate to feeding grounds in the Bering and Chukchi seas in summer. They feed principally on infaunal amphipods (*2*). Although they do feed during migration (*2*), most of their nourishment comes from foraging in the 1 × 10^6 km^2 of Arctic shelf that constitutes their northern feeding grounds (*3, 4*).

Mud plumes in the water column near gray whales are indications of benthic feeding activity (*5*). Such behavior has been observed in a captive gray whale (*6*) and inferred by divers (*7, 8*). The whales use oral suction to rip up patches of amphipod-rich sea floor, then expel the sediment through their baleen and consume the amphipods retained. The resulting pits on the sea floor are of sufficient size and reflectivity to be detected, measured, and mapped by side-scan sonar (Fig. 1) (*9*).

More than 4500 line-kilometers of 105-kHz side-scan sonar data were collected in the northern Bering Sea between 1977 and 1982. The records show high concentrations of feeding pits over a 22,000-km^2 area in the center of the Chirikov Basin and the southern nearshore areas of Saint Lawrence Island. Feeding pits are absent, however, in Norton Sound, the Shpanberg Strait, and immediately north of Saint Lawrence Island (Fig. 2).

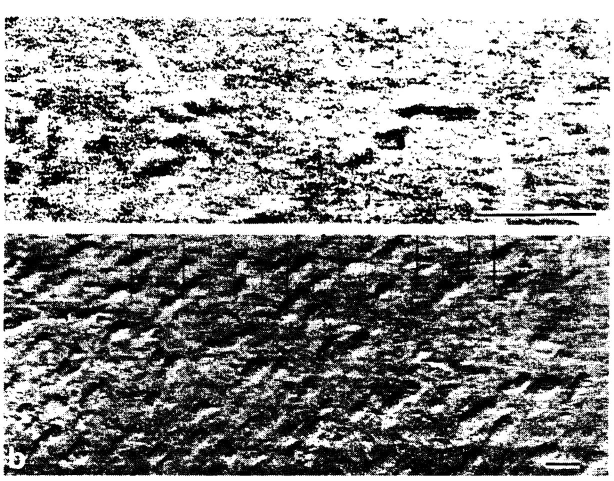

Fig. 1. Side-scan sonographs of the central Chirikov Basin floor, northeastern Bering Sea, showing (a) multiple fresh whale feeding pits and (b) older pits enlarged and oriented by the current. Scale bars, 10m.

In the northern Bering Sea the main prey of the gray whale is probably the tubicolous amphipod *Ampelisca macrocephala* (*10*), which is found in a substrate of very fine (0.125 mm), well-sorted sand (*11*). Abundant amphipod tubes commonly coalesce to form a mat that effectively fixes the sediment surface and protects it from scouring by the current (*12*). The ampeliscid amphipod distribution (*13*) closely matches the distribution of whale feeding pits and aerial sightings of feeding gray whales (Fig. 2) (*5, 14*).

The widespread amphipod substrate was deposited at the end of the latest glacial maximum (12,000 to 10,000 years ago), when melting ice caused a marine transgression over the Bering Land Bridge. Beach sand and gravel were laid down first over the silty tundra peat of the land bridge (*15*). Then a thin (<2 m) sheet of inner-shelf fine sand was deposited. Recent input from the Yukon River has covered Norton Sound with silt and fine sand, and strong currents of the Shpanberg Strait have reworked the sediment there into coarser lag deposits. Thus only the Chirikov Basin is floored by a relict, laterally extensive sheet of homogeneous fine sand that provides the amphipod habitat (Fig. 2).

Modern processes are highly active in modifying the Bering Sea floor. The northern Bering Sea is icebound for half the year, resulting in a winter quiescence under the ice cover, except in areas where shearing ice packs cause scouring of the sea floor (*16*). Spring ice breakup (*17*) is followed by a midsummer calm. A storm season in the fall results in the triggering of gas expulsion craters (*18*), extensive scouring by currents (*19*), and high rates of sediment transport (*20*).

The whale feeding pits vary in size, shape, and density. Much of this variation can be explained as modification after formation by sediment infilling, by further feeding activity, or by current-scour enlargement. Fresh, unmodified pits seem to be oval, 0.5 to 4.0 m long, 0.5 to 2.0 m wide, and 0.1 to 0.4 m deep. They commonly occur in organized, linear, or radial groups of two to eight or more, and apparently are created by multiple feeding events (Fig. 1a) (*2, 9*). Apparently, whales can also create pits while swimming or drifting with the current because some pits are as long as 8 m, though still of normal width.